

## Computer Model for Automobile Climate Control System Simulation and Application

Öner ARICI and Song-Lin YANG  
Mechanical Engineering and Engineering Mechanics  
Michigan Technological University  
1400 Townsend Drive, Houghton, MI - USA 49931-1295  
Phone: (906) 487 2089, Fax: (906) 487 2822  
E-mail: arici@mtu.edu

Daniel HUANG and Emin ÖKER  
Visteon Climate Control Systems Division  
45000 Helm Street, Plymouth, MI - USA 48170  
Phone: (734) 451 9049, Fax: (734) 451 8848  
E-mail: dhuang2@visteon.com

### Abstract

A software to simulate the dynamic operation of climate control system for a generic automobile has been developed. The transient nature of passenger cabin temperature and relative humidity are predicted using the principles of thermodynamics. Analysis include detailed simulations of every component of the automobile air conditioning network. The methodology is validated by comparing the simulation results with the experimental results.

*Key words: dynamic air conditioning system simulation, climate control, passenger vehicles*

### 1. Introduction

Traditionally, development of a prototype system in the auto industry requires extensive and expensive wind tunnel testing before the design enters the production line. Car manufacturers are therefore looking for ways to improve competitiveness by reducing the number of time consuming prototype tests. Combining the use of theory, simulations, and limited number of experimental data has been proven to be successful over the years and is therefore recognized as a modern tool by the designers. The software presented will help minimize the costly and time-consuming procedures to integrate a prototype air conditioning (A/C) system to desired climate objectives.

The paper will be presented in two parts; Part I will be limited to A/C circuit only and the remaining part, Part II will address climate modeling of the passenger space.

### 2. Part I: A/C System Simulation

The goal of this part is to present a computer model to simulate the dynamic features of

an automotive A/C system under realistic conditions (idle, highway, city traffic, etc.).

The mathematical modeling for the individual components will be presented first. The transient simulation models of the air handling system (or ventilation system) including blower and air ducts will also be described. Finally, the methodology developed for dynamic simulation of an automotive A/C circuit will be addressed in detail.

#### 2.1 Compressor model

In the earlier studies (Cherng 1989, Davis 1972) the compressor was modeled based on a reversible compression process of an ideal gas with constant specific heats. An alternative approach recommended here is that the compressor is modeled numerically using first and second laws of thermodynamics coupled with compressor characteristics. Compressor characteristics are those for isentropic efficiency and the volumetric flow rate. They were generated from compressor test data in terms of compressor speed and compression ratio. Given the refriger-

ant inlet enthalpy and compression ratio, refrigerant mass flow rate and the outlet enthalpy can now be calculated using these characteristics.

## 2.2 Orifice tube model

The main function of the orifice tube (capillary tube) is to regulate the flow rate of the refrigerant and to throttle it to the evaporator suction pressure level. The flow rate across the orifice tube is controlled by tube size and length, pressure difference between the inlet and the outlet, and the degree of inlet subcooling. The orifice tube model developed in this study was based on the standard definition of flow in capillary tube (White 1994).

$$\dot{m}_0 = C_d A_0 \sqrt{2\rho_{in}(p_{in} - p_{out})} \quad (1)$$

The discharge coefficient  $C_d$  was obtained experimentally and provided by the sponsor. Other variables are described in the nomenclature section. The state of the refrigerant leaving the orifice tube with the given values of the inlet refrigerant enthalpy and the outlet pressure is based on the isenthalpic flow assumption.

The results of the predicted orifice tube behavior were verified against experimental data, and shown in TABLE I.

TABLE I. Predicted Flow Rate Across Orifice Tube.

Dia. (m)	$P_{in}$ (bar)	$P_{out}$ (bar)	Sub-cooling (°C)	Calc. Flowrate (gm/s)	Test Flowrate (gm/s)	Error (%)
9.58 E-4	13.7	2.8	29.2	25.297	23.951	5.620
9.58 E-4	25.6	4.8	13.2	23.614	21.899	7.831
1.821 E-3	29.0	11.9	15.6	89.497	85.458	4.726
1.821 E-3	25.2	10.1	8.0	67.923	64.955	4.569

## 2.3 Evaporator model

The geometry of the evaporator in this study is a plate-fin type of evaporator which is used widely in automotive A/C systems.

Simulation of the evaporator to conveniently describe the operation under all circumstances requires the study of heat transfer, pressure drop in the single-phase as well as two-phase regions including the evaporator geometry and the thermal inertia of the core material. The majority of research work (Davis 1972, Cherg 1989, Kyle 1993, Castro 1993, Ali 1995, Khamsi 1997, and Selow 1997) for the evaporator simulation was completed using the steady-state effectiveness NTU method (Kays 1984). However, this is not deemed to be an appropriate methodology for the objectives of this study.

A transient model (Huang 1998) takes into account the "local" influences on the heat transfer and pressure drop, temperature, and phase change at the refrigerant side. Along the direction of the refrigerant flow, the evaporator is

divided into a number of smaller control volumes, or elements, to evaluate the local heat transfer and pressure variations within the segment. When the flow conditions are specified at evaporator inlet and the initial conditions are given, the calculations for a small control volume proceed in the refrigerant flow direction until it reaches the evaporator exit as depicted in Figure 1.

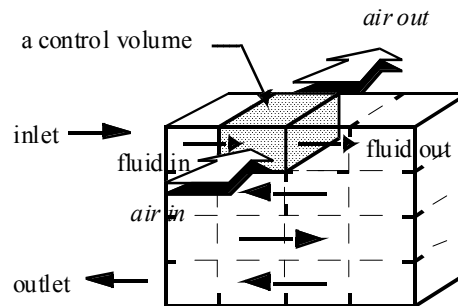


Figure 1. Control volume model of evaporator

A small element of a cross-flow evaporator with fins is shown in Figure 2. The fins and flow channels are lumped to effectively yield an individual metal tube with the refrigerant flowing in the interior and air passing over the exterior

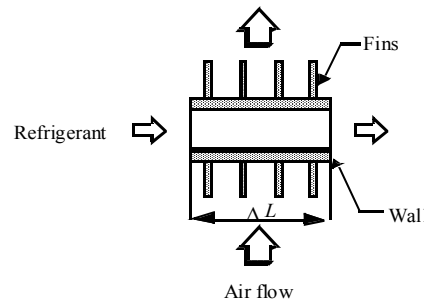


Figure 2. Evaporator element.

## 2.4 Governing equations

The conservation of energy applied on the evaporator wall, refrigerant, and the returning air in each element yield a set of three coupled differential equations (Chiang 1995).

Metal:

$$\rho_w V_w c_w \frac{dT_w}{dt} = h_r A_r (T_r - T_w) + h_a A_a \eta' (T_a - T_w) \quad (2)$$

Refrigerant:

$$\rho_r V_r \frac{di_r}{dt} = \dot{m}(i_{r,i} - i_{r,0}) + h_r A_r (T_w - T_r) \quad (3)$$

Air:

$$\rho_a V_a c_a \frac{dT_a}{dt} = \rho_a A_a U_a (T_{a,i} - T_{a,0}) + h_a A_a \eta' (T_a - T_w) \quad (4)$$

Heat transfer coefficient and pressure drop correlations are based on Dittus-Boelter (Özsisik 1985) and Darcy-Weisbach (White 1994) for single-phase, Chen (Özsisik 1985) and Chisholm (Hewitt et al. (1994) for two-phase fluids respectively. The air-side heat transfer and pressure drop were calculated from the experimental data provided by Kays and London (1984). The computer implementation requires that values for initial air pressure and temperature, initial refrigerant pressure and temperature, refrigerant inlet pressure, enthalpy and flow rate, air inlet pressure, temperature, and evaporator configuration are given at the start. Optimum time step size was determined through numerical experimentation.

It is important to note that in this study evaporator was considered “dry” for convenience and speed of calculations. Therefore mass transfer between the evaporator coil surface and the air; and the water film resistance and its effect on the heat transfer and the pressure drop were neglected. While wet evaporator is scientifically correct mode of operation, the prediction of the state of conditioned air coming out of the evaporator was within acceptable error margin and was not deemed essential at that stage. The “wet” evaporator model is under evaluation and the improvements to the code will be made available later.

### 2.5 Condenser model

The geometry of the condenser in the present study is a high capacity parallel-flow type condenser frequently used in automotive air-conditioning systems. It consists of multiple passages for refrigerant flow and finned cross-flow passages for air. A transient mathematical model similar to that of evaporator was developed to calculate the condenser performance with the given geometry and pre-specified refrigerant and air inlet conditions. The governing equations used are the same as those used for the evaporator. The air-side heat transfer coefficient was based on the correlations proposed by Kays and London 1984. For the two-phase condensing region, heat transfer coefficient was calculated using correlation recommended by Akers et al. (Özsisik 1985).

Along the direction of the refrigerant flow a condenser is divided into a number of small elements. The elements are not necessarily the same because of unequal number of flow channels, as shown in *Figure 3*. Each segment is treated as a separate heat exchanger element and the amount of heat transfer and refrigerant pressure drop in that segment is calculated with the corresponding correlations.

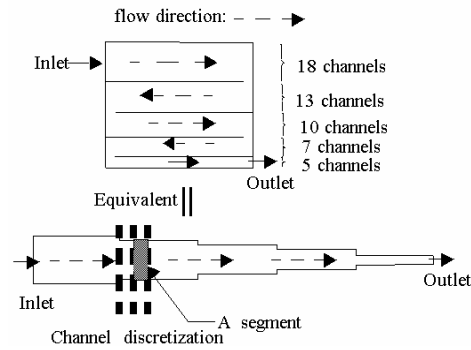


*Figure 3. A real condenser and an equivalent horizontal tube condenser.*

### 3. Air Handling System

In the automotive applications, air ducts are usually exposed to hot environment such as the instrument panel (IP) or engine compartment. The heat from the engine block and the solar radiation transmitted through the windshield cause the IP unit and the space beneath to achieve high temperatures. The hot environment causes the air in the ducts gain heat after leaving the evaporator core before reaching the registers. The state of air entering the passenger compartment is crucial to the HVAC system design, and it is an important input parameter to the calculations of cabin temperature and humidity. It is therefore essential that a realistic assessment of the air in the registers be made under transient state. Air handling system model in this analysis is considered to include two submodels, one for blower and the other for air-duct network.

To evaluate the blower performance; the pressure rise and power input to blower operating at a temperature different from test condition, the relationships among these performance parameters are established through fan laws (ASHRAE 1996) based on supplier provided characteristics.

For transient internal flows it is desired to predict pressure variations and heat transfer between the wall and the fluid using standard conservation laws. Utilizing the discretized control volume approach to model air ducts, the net effects of the pressure losses and heat transfer are obtained by summing up the local variations for each single element.

The air ducts were appropriately divided into several control volumes when needed to resolve complex geometries. Based on the first law of thermodynamics, the three governing equations for the duct, the internal fluid, and the ambient air were derived similar to evaporator model (Huang 1998).

The heat transfer coefficient for internal flows are readily available in any standard text-

book. Convective heat transfer coefficient externally were predicted as cylinder in cross flow under prevailing external state of air; forced or natural. The pressure losses in the duct and duct fittings were determined using Darcy-Weisbach equation (White 1994), combined with the experimental loss coefficients and expressed in a single equation below.

$$\Delta p = \frac{\rho U^2}{2} \left( \frac{f \Delta L}{D_h} + \sum K_i \right) \quad (5)$$

With known boundary conditions and geometric profiles for the air ducts, the system resistance to the air flow caused by the duct network, evaporator coil, etc. can be calculated through air handling system submodel. The system resistance is then used to determine the system volumetric flow rate at any instant of time during simulations. The air flow rate is the operating point at which the system pressure loss, given by Equation 5, is just balanced by the pressure head developed by the blower.

In a similar fashion, refrigerant hoses were divided into small elements to account for the local variations of temperature and pressure.

#### 4. A/C System Integration

From the mathematical point of view, there are three parameters needed to describe a refrigeration loop, *Figure 4*. They are; the discharge pressure (or high-side pressure), the suction pressure (or low-side pressure), and the refrigerant flow rate. These parameters vary if operating conditions change in any of the A/C unit component and are essential constraints which must be provided to determine a specific refrigeration loop.

In general, the balance point for the A/C system is defined as the point at which the high-side flow rate pumped by compressor exactly equals the low-side flow rate restricted by the orifice tube. Consequently, the design characteristics of the compressor and orifice tube serve as two independent constraints to the refrigeration cycle. The other constraint comes from the refrigerant inventory balance. At any instant of time the total refrigerant mass stored in the components and connecting lines must equal the initial refrigerant mass charged into the system. However, predicting refrigerant inventory in the components, especially in the two-phase flow region, is a very complex task and was not the goal of the study presented here. Research in this area has not fully matured due to the uncertainties involved in the void fraction correlations. For the sake of simplicity, and computational expediency a reasonable compromise was proposed to supply an alternative constraint; the refrigerant state at the evaporator exit.

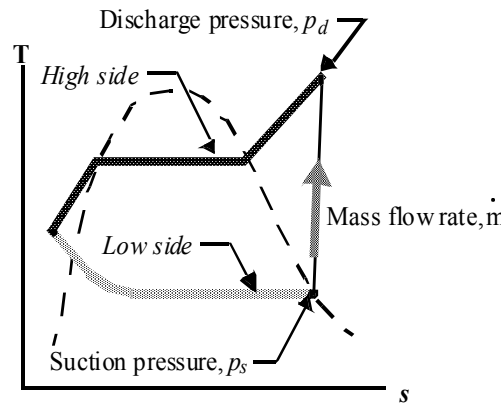


Figure 4. Refrigeration loop - constraints

#### 4.1 Solution algorithm

An effective computer algorithm along with the stable numerical method is required to achieve a balanced refrigeration loop from the design characteristics of components and their operating conditions. The flow chart in *Figure 5* shows the principal steps used to integrate a complete A/C system.

The compressor model first uses initial guesses of the current discharge and suction pressures and an assumption of refrigerant state (enthalpy) at the evaporator exit to calculate refrigerant high-side flow rate and exit enthalpy. After the refrigerant state is updated due to heat and pressure losses in the connecting hoses, the condenser model then calculates the refrigerant state leaving the condenser as a function of flow rates and states of the entering refrigerant and the external air. The orifice tube model then uses inlet refrigerant state and the current suction pressure to calculate the low-side flow rate through the orifice tube. The discharge pressure is being updated until the two flow rates match to within a specified tolerance. Afterwards, the algorithm moves to the evaporator model.

The evaporator model determines exit state of the refrigerant based on the inlet state, converged flow rate, and return air stream flow rate and properties across the evaporator. Since the refrigeration loop is a closed system, the refrigerant enthalpy at the evaporator exit, where calculations start and end, must remain the same after a cycle loop is completed. The estimate in suction pressure keeps improving until the enthalpies converge at the evaporator exit. When both the flow rate and the refrigerant enthalpy at evaporator exit converged, the refrigeration cycle is said to be balanced. Note that the real fluid and thermal effects along the interconnecting hoses are also accounted for in the A/C system integration.

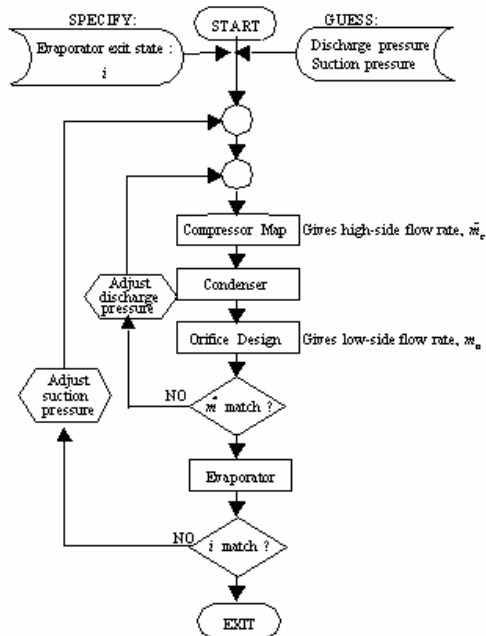


Figure 5. Flow chart for system integration.

The numerical method used in the current research is the shooting method (Chapra 1988). It is based on converting the boundary-value problem into an equivalent initial-value problem by assuming a sufficient number of initial values.

## 5. Experimental Verification

To validate the simulation models presented, tests were carried out for a light truck with a single A/C unit. The schematics of HVAC system for this vehicle are illustrated in Figure 6.

During wind tunnel testing, the vehicle is initially soaked by use of heating panels on the roof until the inside air temperature in the passenger cabin reaches to 60°C while the ambient temperature is held constant at 43.3°C. At time zero, the vehicle begins to move at the speed of 30 mph (miles per hour) during the first 30 minutes. The speed is then increased to 40 mph in the next 30 minutes, and then up to 60 mph in the following 30 minutes before the vehicle is brought to full idle at 5401 seconds. After that the vehicle is maintained at idle for the remainder of the test, for another 30 minutes.

The models were verified by comparing computer-simulated results with the wind tunnel test data. Figures 7, and 8 show the comparisons of predicted average air temperature at the evaporator outlet, and front panel registers outlet with the experimental measurements. Since the cooled air leaving the evaporator picks up heat in the supply air duct as it approaches the registers, the temperature shown in Figure 8 is slightly higher than that in Figure 7.

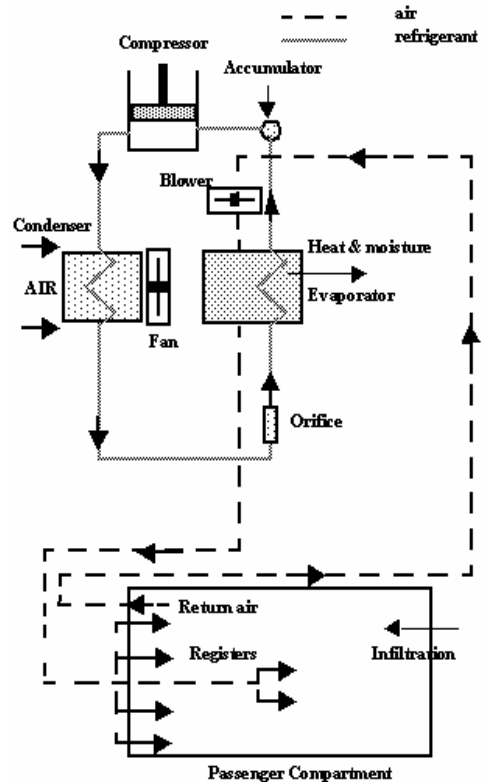


Figure 6. A/C system circuit

## 6. Part II: Climate Control Modeling

In general, there are four environmental properties which impact human comfort: dry bulb temperature, relative humidity, air velocity, and the mean radiant temperature, and all vary in time. An acceptable range of temperature and relative humidity for a person in summer clothing pursuing mainly sedentary activity would be between 24°C to 27°C and 30% to 70% relative humidity. Most of the relevant work in the area of in-car climate control do not take into account the effects of humidity on either the passenger comfort or on the calculated interior temperature. The model presented here predicts both the transient dry bulb temperature and relative humidity.

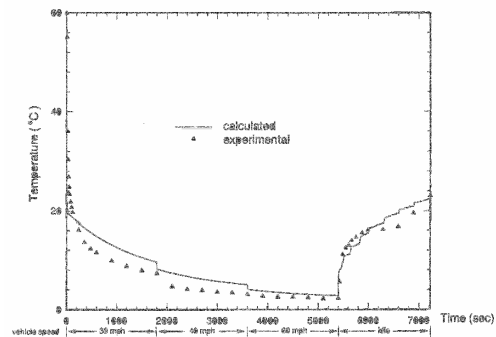


Figure 7. Air temperature at evaporator outlet.

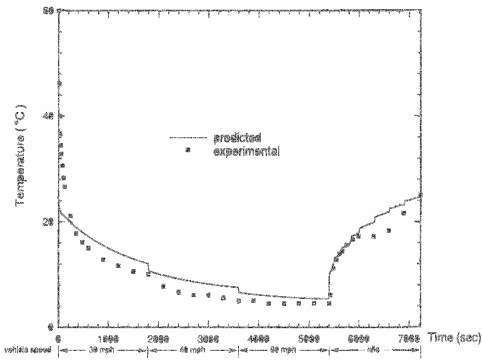


Figure 8. Front panel register air temperature.

Among available literature, thermal load calculations were usually performed without considering the vehicle heat storage effect. However, it is essential that heat capacity of the external and internal structures be included in the analysis since they act as a major heat source during the first 10 minutes of A/C pull-down during testing. Table 2 compares the present model other available models.

Davis (1972) and Cherng (1989) studied the climate control of an automotive vehicle by simulating the components of the A/C unit and then integrating the evaporator air output to the passenger compartment to determine the air temperature variations. The passenger compartment was simulated using a lumped three-dimensional zonal approach using the thermal resistance concept between the zones. Kohler (1990) investigated the transient humidity and temperature responses of a bus with a capacity of 50 persons. Lumped HVAC system simulation is integrated into their model. Reported predictions and experiments are in good agreement. Experiments were limited to a period of one hour while the vehicle was at rest under solar loading. Bos (1993) for the first time simulated automotive passenger compartment climate using a lumped system approach. However, the thermal loads were estimated based on the steady-state vehicle shell structure discounting the transient thermal inertia. Eisenhour (1996) described in-cabin heat flux with a steady-state energy balance equation that accounts for the thermodynamic interactions between the interior temperature, outlet temperature, and the interior air flow. Stancato and Onusic (1997) developed a simulation model to calculate the steady-state heat loads in the cab. The heat loads included solar radiation through glasses, conduction through the body walls and glasses, conduction through the motor compartment, fresh air intake/infiltrations, passengers and equipment.

TABLE II. Comparison of Available Models.

Author	Passenger Compartment Model	
	Heat Storage Effect	Relative Humidity Modeling
Huang et al. (1998) (current model)	yes	yes
Stancato et al. (1997)	none	none
Khamsi et al. (1997)	none	yes
Selow et al. (1997)	none	yes
Eisenhour (1996)	none	none
Bos (1993)	none	yes
Kohler et al. (1990)	none	yes
Cherng et al. (1989)	none	none
Davis et al. (1972)	none	none

The vehicle passenger compartment model presented here was developed using lumped system approach. The variations of the temperature and relative humidity are calculated based on the vehicle transient heating/cooling conditions, such as solar load over opaque surfaces and through the windows, convective and conductive heat loads toward the cabin, passenger heat and moisture loads on the interior air, and the A/C unit conditioned air into the volume. For validation the simulation results are compared to the experimental data.

## 7. Vehicle Thermal Load Evaluation

The solar load on the vehicle's exterior surfaces is calculated using the anisotropic HDKR model proposed by Reindl et al. (Duffie 1991). It should be noted that although proposed thermal load seems to be in agreement with test data available from wind tunnel simulations, more validation against outdoor field data would be needed.

The net energy absorbed by the opaque surfaces of the vehicle exterior is determined by balancing solar radiation to the surface by emission to environment, convective/radiative loss (or gain) externally, conduction toward the vehicle, convection/radiation internal. The vehicle exterior under solar radiation is at a higher surface temperature than that of interior. High surface temperature naturally results in higher heat loads to the vehicle.

Solar radiation, which passes through the glasses and incidents on the vehicle interior surfaces, is modified by an appropriate manufacturer supplied transmittance-absorptance product.

## 7.1 Passenger heat and moisture load

The heat and moisture load from the passengers is a very complex issue. Since the thermoregulatory system of the body will maintain an essentially constant internal body temperature, it can be assumed that a heat balance will exist for the human body for long exposures to a constant thermal environment with a constant metabolic rate. Therefore, the heat generation will equal the heat dissipation, and there will be no significant heat storage in the body.

The model that describes the heat and moisture generated from passengers to the ambient inside the cabin are developed based on the methodology described by Fanger (1970). This model assumes that under thermal equilibrium and negligible heat storage within the body heat added to the air from passengers is contributed by sensible heat loss from skin and by sensible respiratory loss. It also allows specification of passenger variables such as height, weight, clothing level, and activity type.

Moisture load generated by humans is considered from respiration, sweating, as well as from the natural diffusion of water through the skin. Each term is calculated separately with appropriate empirical correlations. The increase in human moisture load on the vehicle interior will cause the value of the cabin relative humidity increase if not adequately controlled, and bring about an uncomfortable environment for the passengers.

## 7.2 Vehicle heat load

The thermal loads on a vehicle are those of the convective and conductive heat loads, which do not include the heat load from the passengers, solar radiation striking the exterior surfaces and passing through the windows of the vehicle. The solar radiation on the individual surface serves as a source term when calculating the convective and conductive heat loads.

The amount of heat load on the vehicle varies with the changes in the boundary conditions imposed on both the exterior and interior surfaces; the surface temperature, air velocity, and solar radiation.

The vehicle considered in this investigation is a light truck. The primary volume of interest is the passenger compartment. To simplify the vehicle model, it is appropriate to consider that a passenger compartment has six sides: top, bottom, front, rear, driver side, and passenger side. Each side consists of several surface elements, and each surface element typically consists of one layer for a glass surface or up to as many as five layers for the rest.

A surface element on a particular side is set up as a rectangle or an equivalent rectangle for otherwise different surface shapes. The thermal properties of a surface and its subsequent layers are assumed to be uniform and are of the same material and thickness. Each surface element will be defined by several parameters including direction, slope, internal and external conditions such as temperature, and air velocity, as well as structure and material characteristics.

During the wind tunnel testing, the passenger space is essentially at a different temperature from those of the environment and the engine cell. At the beginning of the simulation, the vehicle is at steady state where the air temperature inside the passenger volume is 60°C, and the ambient temperature is constant 43.3°C. Conductive and convective heat loads to the cabin are determined by the external air temperature, the vehicle speed, the varying interior temperature, coupled with the heat capacity of the car shell.

To account for the transient heat capacity of surface elements, each surface element is considered as a composite slab. The thickness of a slab is much less than the length and the width of the slab. It is then reasonable to assume that temperature varies only in the x-direction along the surface normal. The general one-dimensional transient heat conduction equation which governs the physical process of interest here is given by

$$\rho c \frac{\partial T}{\partial t} = \frac{\partial}{\partial x} \left( k \frac{dT}{dx} \right) \quad (6)$$

It is assumed that thermal properties (conductivity, density, specific heat, etc.) and temperature are uniform within each individual layer or control volume. Thus, for each control volume there is only one grid point which denotes its homogeneous properties. The number of grid points is created in response to the number of layers plus two boundary points in each surface element. For example, five grid points are required to represent a three-layer surface element.

The numerical scheme adopted to discretize Equation 6, was that of Patankar (1980). To evaluate the heat load on a surface element, the surface temperatures at the boundary nodes must be computed. The surface temperatures are obtained through a discretized equations by marching in time from the given initial temperature distribution and the boundary conditions. The boundary condition values are those of solar radiation, heat transfer coefficients on the exterior and interior sides. Note that the interface conductivities in the composite wall are carefully evaluated by linear variation between two adjacent grid points.

To simplify the calculation, the algorithm will compute current heat loads based on the heat transfer coefficients obtained at the previous time step. With knowledge of the interior surface temperatures and cabin temperature the total convective heat load to the passenger space is hence obtained by summing up the thermal loading on every surface element. This conductive/convective heat load plus the solar and human loads are then used in the lumped transient analysis as the source terms to calculate the passenger compartment temperature and humidity variations.

### 7.3 Lumped system model

To perform system benchmark comparison and parametric study it is unnecessary to develop a computer simulation tool. The passenger compartment was analyzed using the lumped capacitance method. It is assumed that the temperature and humidity inside the passenger compartment is spatially uniform at any instant of time during the process. This assumption implies perfect mixing of the air inside the compartment at all time. In addition, a lumped analysis of the interior masses (seats, IP, floor console, etc.), which act either as a heat source or heat sink, is included in the analysis.

The flow of energy and air in and out of the passenger compartment is described by four coupled nonlinear ordinary differential equations. These equations are based on dry air mass balance, vapor mass balance, interior air energy balance, and cabin interior mass energy balance.

Air enters the vehicle from two sources, infiltration and the air conditioner. Air exits the vehicle only by return air vents. The air entering and exiting the vehicle carries with it a certain amount of moisture. While the moisture enters the vehicle through infiltration, conditioned air. It is also added to the system by passenger perspiration and respiration. These sources provide the basis for mass balance of both dry air and vapor.

### 7.4 Energy balance equations

The energy rate equations one for air and other for the cabin interior masses are expressed through conventional means (Huang 1998). It is more convenient however to formulate the above differential equations in terms of temperature and humidity ratio, so that the final forms would contain the desired variables and are readily solved by applying appropriate numerical methods.

Three coupled non-linear equations are now obtained in terms of the cabin air temperature  $T_p$ , the cabin air humidity ratio  $w$ , and the interior equivalent mass temperature  $T_m$ .

$$\frac{dw}{dt} = \frac{A}{\dot{m}_a} \quad (7)$$

$$\frac{dT_p}{dt} = \frac{B - A(2501 + 1,805T_p)}{\dot{m}_a (1 + 1,805w)} \quad (8)$$

$$\frac{dT_m}{dt} = \frac{[(1 - \Omega)\dot{Q}_s - hA_m(T_m - T_p)]}{(mc)_m} \quad (9)$$

where

$$A = (\dot{m}_a w)_i + (\dot{m}_a w)_{AC} + \dot{m}_{v,h} - w(\dot{m}_{a,i} + \dot{m}_{a,AC})$$

and

$$B = \Omega\dot{Q}_s + \dot{Q}_c + \dot{Q}_h + \dot{Q}_m$$

Here  $\Omega$  represents the part of solar heat load which is absorbed by the internal masses, the rest is therefore given away to air by means of radiative interactions. Another way would be considering  $\Omega=1$  and adding nonlinear radiative heat transfer component to Equation 9. From the views of computational expediency and the objectives in mind the first lumped model has been chosen.

It should be noted that interior masses have been lumped into one, with a temperature, heat capacity, exposed area, and heat transfer coefficients of  $T_m$ ,  $(mc)_m$ ,  $A$ , and  $h$  respectively. In the analysis the convective coefficient  $h$  has been optimized for better comparisons. The improved model by considering multiple masses such as seats and panels, is under consideration and will be presented later.

Since the relative humidity is also one of the important variables that define human comfort, the designer is therefore interested in the relative humidity rather than the humidity ratio. However, it is the humidity ratio which is required for the solution of the governing equations.

## 8. Numerical Method Implementation

The Equations, (7), (8) and (9), were solved simultaneously using a classical fourth-order Runge-Kutta method with step size control (Chapra 1988). The water vapor contributed from human, infiltration, and A/C cooling air were considered and calculated separately. The current ( $n+1$  step) values of average humidity ratio as well as temperature are calculated based on the values of both humidity ratio and temperature at the previous time step ( $n$  step). The removal of moisture is handled automatically in this explicit algorithm. The return air (at  $n$  step) leaving the passenger compartment carries the moisture to the evaporator, where it condenses and moisture content is reduced. Then, the evaporator model uses this return air information (at  $n$  step) to calculate the current ( $n+1$  step) value of conditioned air humidity ratio and temperature, which are now the input parameters for the calculations of passenger compartment humidity ratio and temperature (at  $n+1$  step).

Note that the concept used for the step size control is to take local truncation error as the difference between two predictions using the Range-Kutta method with different step sizes. The difference in these two calculations represents an estimate of the local truncation error. If the error is too small, the algorithm would increase the step size, or decrease it if the error is too large. This adaptive computational scheme has been proven to be a successful way to reduce CPU time by one to two orders while still yielding satisfactory results

## 9. Results And Discussions

Figure 9 presents the predicted/experimental interior average air temperature profile as a function of time for a baseline vehicle. As the vehicle speed increases, the interior air temperature uniformly drops toward a steady state value due to the surge of conditioned air into the volume. The overall trends of the calculated results are consistent with the experimental data with an error margin of 5% error.

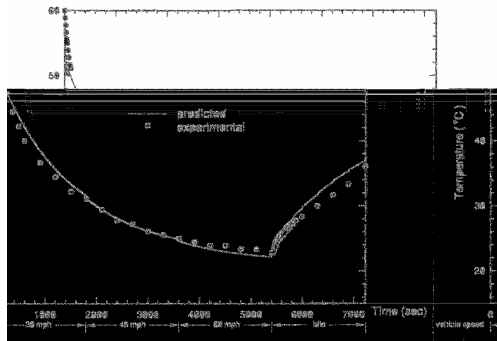


Figure 9. Vehicle interior air temperature

The predicted relative humidity inside the cabin is shown in Figure 10. Initially, the cabin is assumed to have a relative humidity of 35% and the ambient is pre-defined to have a constant value of 65% over time. During the first 100 seconds, the variation of relative humidity shows a rise to a value of about 38% (not shown because of fine scale) due to the sharp drop in interior temperature after the A/C unit is switched on at time zero. After 300 seconds, the humidity distribution is relatively steady. This is expected and is also consistent with the experimental data presented by Kohler 1990. Unfortunately, there is a shortage of experimental data regarding the transient relative humidity in the passenger compartment. The rate equations for the temperature and humidity ratio are coupled, since the temperature predictions are accurate it is tempting to assume that the relative humidity value predictions are also within an appropriate range.

The model is used next for parametric study which enable the designer to achieve optimum

design objectives without even testing an actual vehicle.

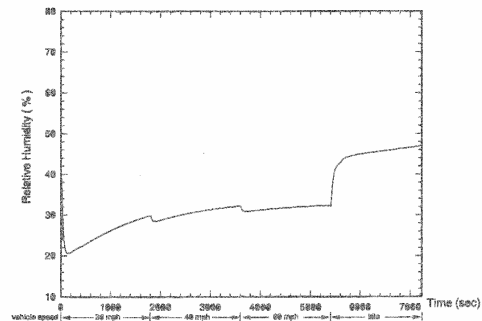


Figure 10. Vehicle interior relative humidity.

A parametric study under various glass type selection is shown in Figure 11. Previous simulations were for a glass type of *privacy*. Simulations are for various other types where front, driver, and passenger side were kept as tinted. These simulations show that solar-reflective glass and a larger blower (not shown) will effectively improve the comfort level of the vehicle interior.

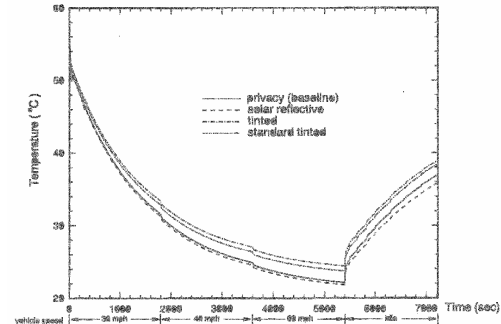


Figure 11. Air temperature-glass type variation.

## 10. Summary

A software package has been developed for the design and simulation of an Automotive Climate Control System. The methodology introduced allows the designer to test the effects of design, component, and structural changes on the temperature and moisture variations of the passenger compartment. This software package aims minimizing the costly and time-consuming procedures for integrating a prototype A/C system.

## Acknowledgment

The authors gratefully acknowledge the sponsorship of Visteon Climate Control System Division. Special thanks also go to Mr. Bin Hong and Dr. David Zietlow for their assistance in collecting the test data used for model validation and their valuable comments on A/C system model development.

## Nomenclature

A	area (m <sup>2</sup> )
c	specific heat (kJ/kg-K)
C <sub>D</sub>	discharge coefficient
D	diameter (m)
f	friction factor
h	heat transfer coefficient (W/m <sup>2</sup> -K)
i	specific enthalpy (kJ/kg)
k	thermal conductivity (W/m-K)
K <sub>i</sub>	minor loss coefficients
$\dot{m}$	mass flow rate (kg/s)
p	pressure (N/m <sup>2</sup> )
$\dot{Q}$	heat transfer rate (kW)
T	temperature (K)
t	time (s)
U	fluid speed (m/s), overall heat transfer coefficient (W/m <sup>2</sup> -K)
V	volume (m <sup>3</sup> )
w	humidity ratio
$\rho$	density (kg/m <sup>3</sup> )
$\eta'$	area-weighted fin efficiency
$\Omega$	defined in Equation (9)

## Subscripts:

AC	air conditioning unit
a	air
c	compressor, also convective
h	hydraulic, human
in or i	inlet, also infiltration
m	interior equivalent mass in the cabin
o	orifice tube
out or o	outlet
p	passenger cabin
s	solar
v	vapor
w	evaporator
r	refrigerant

## References

- Ali, A. A., R., Castro, F., Tinaut, F. V., and Melgar, M., 1995, "Modelling of Automotive Air Conditioning Parallel Flow Condensers with Pressure Drop Calculations," IMechE 954052.
- ASHRAE, 1996, *ASHRAE Handbook, Systems and Equipment*, ASHRAE.
- Bos, J. A., 1993, "A Computer Model for Automobile Passenger Compartment Climate Control," M.S. Thesis, Michigan Technological University, Houghton, Michigan.
- Castro, F., Tinaut, F. V., and Ali, A. A. R., 1993, "Automotive Evaporator and Condenser Modeling," SAE Paper 931121.
- Chapra, S. C. and Canale, R. P., 1988, *Numerical Methods for Engineers*, 2nd Edition, McGraw-Hill, New York.
- Cherng, J. G. and Wu, W. J., 1989, "Design Tool for Climatic Control of an Automotive Vehicle," SAE Paper 891966.

Chiang, E. C. and Ng, S. Y. C., 1995, "Computer Simulation of Refrigerant Vapor Condenser in Transient Operation," SAE Paper 951014.

Davis, G. L., Chianese, F. Jr., and Scott, T. C., 1972, "Computer Simulation of Automotive Air Conditioning - Components, System, and Vehicle," SAE Paper 720077.

Duffie, J. A., Beckman, W. A., 1991, *Solar Engineering of Thermal Processes*, 2nd Edition, John Wiley & Sons, Inc.

Eisenhour, R., 1996, "Automatic Climate Control Equation for Improved Heat Flux Response," SAE Paper 960683.

Fanger, P. O., 1970, *Thermal Comfort*, McGraw-Hill, Inc.

Hewitt, G. F., Shires, G. L., Bott, T. R. 1994, *Process Heat Transfer*, CRC Press, Inc.

Huang, D.C., 1998, "A Dynamic Computer Simulation Model for Automobile passenger Compartment Climate Control and Evaluation," Ph.D. Thesis, Michigan Technological University.

Kays, W. M. and London, A. L., 1984, *Compact Heat Exchangers*, 3rd Edition. New York, McGraw-Hill.

Khamsi, Y., Mathey, F., and Pomme, V., 1997, "Modeling of Automotive Passenger Compartment and its Air Conditioning System," SAE Paper 971783.

Kohler, J., Kuhn, B., Sonnekalb, M., Beer, H., 1990, "Numerical Calculation of the Distribution of Temperature and Heat Flux in Buses under the Influence of the Vehicle Air-Conditioning System," *ASHRAE Trans.*, Vol. 96, Part 1, pp. 432-446.

Kyle, D. M., Mei, V. C., and Chen, F. C., 1993, "An Automobile Air Conditioning Design Model," SAE Paper 931137.

Orth, L. A., Zietlow, D. C., Pedersen, C. O., 1995, "Predicting Refrigerant Inventory of R-134a in Air-Cooled Condensers," *ASHRAE Trans.*, Vol. 101, Part 1.

Ozisik, M. N., 1985, *Heat Transfer*, McGraw-Hill, New York.

Patankar, S. V., 1980, *Numerical Heat Transfer and Fluid Flow*, McGraw-Hill, New York.

Selow, J., Wallis, M., Zoz, S., and Wiseman, M., 1997, "Towards a Virtual Vehicle for Thermal Analysis," SAE Paper 971841.

Stancato, F., Onusic H., 1997, "Road Bus Heat Loads Numerical and Experimental Evaluation," SAE Paper 971825.

White, F. M., 1994, *Fluid Mechanics*, 3rd Edition, McGraw-Hill, New York.

